

## Annual Research & Review in Biology

23(4): 1-14, 2018; Article no.ARRB.39315  
ISSN: 2347-565X, NLM ID: 101632869

# Postmortem Diagnosis of Induced Fatal Anaphylactic Shock in Rats

Said Said Elshama<sup>1,2\*</sup>, Rasha R. Salem<sup>3</sup>, Hosam-Eldin Hussein Osman<sup>4,5</sup>  
and Ayman El-Meghawry El-Kenawy<sup>6,7</sup>

<sup>1</sup>Department of Forensic Medicine and Clinical Toxicology, College of Medicine, Taif University, Taif, Saudi Arabia.

<sup>2</sup>Department of Forensic Medicine and Clinical Toxicology, Faculty of Medicine, Suez Canal University, Ismailia City, Egypt.

<sup>3</sup>Department of Anatomy, Faculty of Medicine, Alexandria University, Egypt.

<sup>4</sup>Department of Anatomy, College of Medicine, Taif University, Taif, Saudi Arabia.

<sup>5</sup>Department of Anatomy, Faculty of Medicine, Al-Azhar University, Cairo, Egypt.

<sup>6</sup>Department of Pathology, College of Medicine, Taif University, Taif, Saudi Arabia.

<sup>7</sup>Department of Molecular Biology, GEBRI, University of Sadat City, Sadat City, Cairo, Egypt.

### Authors' contributions

This work was carried out in collaboration between all authors. Author SSE designed the study, wrote the protocol and the first draft of the manuscript. Authors RRS and HEHO managed the analyses of the study and the literature searches. Author AEMEK performed the statistical analysis. All authors read and approved the final manuscript.

### Article Information

DOI: 10.9734/ARRB/2018/39315

#### Editor(s):

(1) George Perry, Dean and Professor of Biology, University of Texas at San Antonio, USA.

#### Reviewers:

(1) Samuel Ifedioranma Ogenyi, Nnamdi Azikiwe University, Nigeria.

(2) Diana C. Tapia-Pancardo, National Autonomous University of México, México.

(3) Rohan Ruwanpura, Karapitiya Teaching Hospital, Sri Lanka.

Complete Peer review History: <http://www.sciedomains.org/review-history/23020>

Original Research Article

Received 10<sup>th</sup> November 2017  
Accepted 30<sup>th</sup> January 2018  
Published 5<sup>th</sup> February 2018

## ABSTRACT

Anaphylactic shock is a sudden and serious life-threatening systemic hypersensitivity leading to a rapid, irreversible fatal circulatory collapse. Postmortem diagnosis of fatal anaphylaxis is a very sophisticated task in forensic medicine; it is usually excluded as the cause of death due to lack of autopsy findings. This study aims to find more specific criteria for the postmortem diagnosis of induced fatal anaphylaxis in rats by assessing the levels of total tryptase, histamine,

\*Corresponding author: E-mail: [saidelshama@yahoo.com](mailto:saidelshama@yahoo.com), [saidelshama@gmail.com](mailto:saidelshama@gmail.com);

immunoglobulin E (IgE) and histological changes in the larynx, trachea, lung, heart, and spleen using light and electron microscopes. Sixty adult albino rats were divided into three groups; each group consisted of twenty rats. The first (control) group received distilled water while the second and third groups received a single intravenous dose of ovalbumin and penicillin G, respectively, two weeks after active subcutaneous sensitization. The fatal anaphylactic shock led to a significant increase in the levels of total tryptase, histamine and immunoglobulin E (IgE) along with histological changes in the larynx, trachea, lung, heart, and spleen that vary its severity according to the anaphylaxis cause. Postmortem diagnosis of fatal anaphylaxis depends on multi-factorial criteria that include biochemical, immunological and histological findings.

*Keywords: Diagnosis; anaphylaxis; postmortem.*

## 1. INTRODUCTION

Anaphylaxis is a severe, life-threatening systemic hypersensitivity; it is caused by multiple factors such as drugs, poisons, venoms and food [1]. Anaphylaxis is a spontaneous and dangerous allergic reaction of the body to particular substances, which are called allergens, that lead to the production of antibodies when it enters the body *via* inhalation, ingestion, dermal contact or inoculation [2].

Anaphylactic shock is an unexpected event wherein 75% of the cases do not have a previous history of hypersensitivity [3]; it is an immediate type of hypersensitivity reaction causing a diffuse organ hypoperfusion. Anaphylactic shock is considered a peripheral circulation failure resulting from antigen-antibody reaction in persons sensitized to a foreign material, leading to rapid, irreversible fatal circulatory collapse [4].

Anaphylaxis is considered to be one of the causes of sudden death. It may occur within a short time from the contact with the allergen; it usually appears a few minutes after allergen exposure, i.e. within 15-20 minutes in most cases. Therefore, death may occur immediately or within one or two hours at the maximum [5].

Anaphylaxis usually is excluded as the cause of death because of the lack of specific findings at the autopsy. Until now, most of the published articles have not been able to establish specific postmortem findings in fatal anaphylaxis cases although there is an increasing incidence of anaphylactic death worldwide [6,7].

Postmortem diagnosis of fatal anaphylaxis is a very sophisticated task in forensic medicine because the medico-legal diagnosis of any disease should not depend only on one type of

investigation; instead, it must rely on a cluster of integrated investigations [8,9]. Thus, we need to establish scientific criteria based on the morphological, biochemical and immunological parameters of fatal anaphylaxis for its postmortem diagnosis.

Therefore, the present study aims to establish more specific and accurate criteria for the postmortem diagnosis of induced fatal anaphylaxis in rats. This study assesses the serum levels of mast cell tryptase, immunoglobulin E (IgE) and histamine, and histopathological changes in the larynx, trachea, lung, heart, and spleen using light and electron microscope examinations.

## 2. MATERIALS AND METHODS

Sixty male adult albino rats (weighing 200-300 g) were maintained on a 12-h day and night cycles, and had free access to food and water during the experimental period. They were divided into three groups where each group consisted of twenty rats. The first (control) group received 0.5 ml of distilled water. Every mouse in the second and third group was actively sensitized twice by a single subcutaneous injection of ovalbumin (1 mg) and penicillin G (0.2 ml), respectively with a one-week time interval. One week after the rats' sensitization, a skin test was performed using the sensitizing material to ensure that every mouse had an immediate active hypersensitivity reaction to the injected material. One week after the skin test, the second and the third group received a single intravenous dose of 1 mg ovalbumin dissolved in 0.5 ml of distilled water [10], and 0.2 ml of penicillin G (10.000 IU) [11], respectively. Anaphylactic shock was induced within thirty minutes to three hours after the last injection.

At the end of the experiment, after the occurrence of death, blood samples from the

three groups were taken within 15 to 30 minutes of death. The blood samples were obtained from the right femoral artery; the samples were left at room temperature for 15-30 minutes to clot. The samples were centrifuged at 2000 rpm for 10 minutes at 4°C to remove the clot and separate the serum samples that were stored at -20°C until the assay.

Total tryptase was measured on ImmunoCAP 100 that uses a fluorescent enzyme immunoassay and a unique solid phase to ensure optimal sites for binding of antibodies whereas all processing steps were fully automated to ensure the reliability and reproducibility of the test. Anti-tryptase that binds to ImmunoCAP reacted with the tryptase in the sample. After washing, enzyme-labeled antibodies against tryptase were added to form a complex. After incubation, the unbound enzyme-anti-tryptase was washed and the bound complex was incubated with the developing agent. After stopping the reaction, the fluorescence in the eluate was measured. The response for the sample was compared with the antibody concentrations used for the calibration curve, and then the results were calculated automatically [12,13].

Histamine in the blood was measured by a radioimmunoassay using the succinyl-glycinamide derivatization of histamine (acylated histamine) in the samples to mimic the immunogen used to generate the monoclonal antibody; it is considered one of the most sensitive assays. The assay exhibited a linear response from 0.01 to 5.0 ug/ml of histamine, and the monoclonal antibody used had partial recognition of only N-methylhistamine (other than histamine) [14,15].

Serum immunoglobulin E (IgE) was measured by an ImmunoCAP-specific IgE blood test that was a fluorescent enzyme immunoassay (FEIA) which measured allergen-specific immunoglobulin E (IgE) in the serum; the assay can measure IgE antibodies that are specific to animals, plants and other allergens [16].

At the end of the experiment, after the sacrifice of the first-group rats and the death of the second and third-group rats, the tissues samples from the larynx, trachea, lung, heart and spleen of the rats from the three groups were taken and fixed in 10% neutral buffered formalin. The fixed specimens were trimmed, washed and dehydrated in ascending grades of alcohol, cleared in xylene, embedded in

paraffin, sectioned at 4-6 µm thickness and stained with toluidine blue, haematoxylin and eosin according to the method described in [17].

Ultrastructure studies were performed by using the transmission electron microscope, and the tissue specimens of different organs were prepared by soaking and fixating the specimens in 2.7% glutaraldehyde solution in 0.1 M phosphate buffer for 1.5 hours at 4°C. It was then washed in 0.15 M phosphate buffer (pH 7.2) and post-fixed in 2% osmic acid solution in 0.15 M phosphate buffer for one hour at 4°C. Dehydration was done using acetone. They were then embedded in the epoxy resin Epon 812. The blocks were cut with an ultramicrotome type LKB at 70 nm thickness. The sections were differentiated with the solutions of uranyl acetate and lead citrate for analysis using an electron microscope [18].

## **2.1 Statistical Analysis**

Statistical analysis was performed using SPSS version 17. The data is expressed as mean ± SD and analyses were performed by using one-way analysis of variance (ANOVA) and post-hoc multiple comparisons tests (TUKEY) to investigate the difference between the biomarker levels among the different groups, where a P value of 0.05 was considered statistically significant.

## **2.2 Ethical Considerations**

The most appropriate animal species was chosen for this research. Promotion of high standard care and animal well-being were exercised at all times. An appropriate sample size was calculated using the fewest number of animals to obtain valid results statistically. Painful procedures were performed under anesthesia to avoid any distress or pain that could be inflicted on the animals. Our standards of animal care are consistent with the requirements and standards of international laws and regulations. It was approved by the Institutional Scientific Research Ethics Committee.

## **3. RESULTS**

### **3.1 Biomarker Findings**

Table 1 shows the mean ± SD of anaphylaxis biomarker levels in the different groups of rats. Mean ± SD values of anaphylaxis biomarker levels (Tryptase, immunoglobulin E "IgE" and histamine) significantly increased in the second

group which was sensitized by ovalbumin in comparison to the control group, and the third group which was sensitized by penicillin G at  $P < 0.001$ .

### **3.2 Histopathological Findings Using a Light Microscope**

#### **3.2.1 Laryngeal histopathological findings**

The examination of laryngeal sections of the rats in the first (control) group revealed a normal structure of the larynx (Fig. 1a) with a normal distribution of mast cells around the blood vessels (Fig. 1d). The laryngeal tissues of the rats in the second group which were sensitized by ovalbumin showed severe inflammatory cellular infiltration, epithelial destruction, submucosal gland swelling, and excessive mucous production (Fig. 1b) with a marked increase in the number of mast cells in the surrounding area of the laryngeal blood vessels (Fig. 1e). The laryngeal sections in the rats of the third group which were sensitized by penicillin G showed mild inflammatory cellular infiltration, epithelial thickness, submucosal gland swelling, and mucous production (Fig. 1c) as well as a mild increase in the number of mast cells (Fig. 1f).

#### **3.2.2 Tracheal histopathological findings**

The examination of tracheal tissues of the rats in the first (control) group showed a typical tracheal structure (Fig. 2a) with a classical distribution of mast cells (Fig. 2d). The tracheal tissues of the rats in the second group which were sensitized by ovalbumin showed significant histopathological changes in comparison to the control group; however, the tracheal and laryngeal histopathological changes in the rats of the second group were nearly similar (Fig. 2b) with a marked increase in the different types of mast cells (Fig. 2e). The tracheal tissues in the rats of the third group which were sensitized by penicillin G showed mild histopathological changes in comparison to the second group; however, the tracheal and laryngeal histopathological changes in the rats of the third group were almost similar (Fig. 2c) with a mild increase in the different types of mast cells (Fig. 2f).

#### **3.2.3 Pulmonary histopathological findings**

The examination of the lungs of the rats in the first control group showed a typical structure of

the lung (Fig. 3a) with normal mast cell distribution around the lung blood vessels (Fig. 3d). The lungs of the rats in the second group which were sensitized by ovalbumin showed a severe loss of normal alveolar wall architecture, fragmentation and degeneration of the alveoli, marked collapse of some alveoli and severe dilatation of others, marked thickening of the interalveolar septum, numerous areas of cellular infiltration in the area surrounding the lung bronchioles, and hemorrhagic blood cells in multiple blood vessels (Fig. 3b) with a significant increase in the mast cells around the pulmonary blood vessels (Fig. 3e). The lungs of the rats in the third group which were sensitized by penicillin G showed a lesser number of atrophic broken alveolar walls, slight erythrocyte accumulation between the alveolar cells, lymphatic infiltration inside and in-between the alveoli together with peri-bronchial lymphocyte infiltration and edema (Fig. 3c), and a moderate increase in the number of mast cells (Fig. 3f).

#### **3.2.4 Cardiac histopathological findings**

The examination of cardiac tissues of the rats in the first (control) group showed a normal appearance (Fig. 4a) with normal mast cell distribution around the coronary blood vessels (Fig. 4d). The hearts of the rats in the second group which were sensitized by ovalbumin showed severe damage in the architecture, fragmentation and degeneration in the myocardial fibers along with congestion, and numerous areas of cellular infiltration surrounding the coronary arteries (Fig. 4b) with a remarkable increase in the mast cell number around the coronary blood vessels (Fig. 4e). The cardiac tissues of the rats in the third group which were sensitized by penicillin G showed a mild loss of normal architecture, cardiac muscle degeneration along with cellular infiltration in areas surrounding the coronary arteries (Fig. 4c) and a mild increase in the number of mast cells (Fig. 4f).

#### **3.2.5 Spleen histopathological findings**

The examination of spleen tissues of the rats in the first (control) group showed a classical structure (Fig. 5a) with normal mast cell distribution around the blood vessels (Fig. 5d). The spleens of the rats in the second group which were sensitized by ovalbumin showed hyalinization in the capsule, trabeculae and the central arterioles wall, lymphocytic infiltration,

subcapsular cloudy swelling, severe hemorrhage, congestion and dilatation of splenic blood sinuses in the red pulp, and white pulp atrophy (Fig. 5b) with a significant increase in the number of mast cells around the blood vessels (Fig. 5e). The spleen tissues of the rats in the third group which were sensitized by penicillin G showed mild lymphatic infiltration with a mild congestion and dilatation of splenic blood sinuses in the red pulp, and hyalinization in the wall of the central arterioles (Fig. 5c) along with a moderate increase in the number of mast cells (Fig. 5f).

### 3.3 Histopathological Findings Using an Electron Microscope

#### 3.3.1 Larynx

Examination of the larynges of the control group rats showed a normal ultrastructural appearance (Fig. 1g). The examination of the larynges of the second group rats which were sensitized by ovalbumin showed severe destruction of the epithelium and goblet cells along with severe cellular infiltration in the sub-endothelial lamina propria and marked increase in the total granulated and degranulated mast cells (Fig. 1h). The examination of the laryngeal section of the third group rats which were sensitized by penicillin G showed a mild destruction of the epithelium and goblet cells along with mild cellular infiltration in the sub-endothelial lamina propria and a mild increase in the total granulated and degranulated mast cells (Fig. 1i).

#### 3.3.2 Trachea

Examination of the trachea of the control group rats showed a classical ultrastructural appearance (Fig. 2g). The examination of the trachea of the second group rats which were sensitized by ovalbumin showed severely destructed mitochondria and necrotic nuclei,

damage in the cilia and the goblet cells, and damaged basal cells with a significant increase in the vacuoles and mast cells (Fig. 2h). The examination of the tracheal section of the third group rats which were sensitized by penicillin G showed a mild damage in the ultrastructure of epithelium associated with a mild increase in the mast cells (Fig. 2i).

#### 3.3.3 Lung

Examination of the lungs of the control group rats showed a typical ultrastructural appearance (Fig. 3g). The examination of the lungs of the second group rats which were sensitized by ovalbumin showed collapsed alveoli, degenerated microvilli in the alveolar surface, marked pyknotic nuclei of pneumocytes type II with degenerative changes in the lamellar bodies and a significant increase in the vacuoles and mast cells (Fig. 3h). The examination of the lung sections of the third group rats which were sensitized by penicillin G showed mildly degenerated microvilli of the alveolar surface along with moderately pyknotic nuclei of pneumocytes type II and a mild increase in the mast cells in the surrounding area of the congested blood capillaries (Fig. 3i).

#### 3.3.4 Heart

The examination of the hearts of the rats in the first (control) group showed a normal ultrastructural appearance (Fig. 4g). The examination of the cardiac tissues of the rats in the second group which were sensitized by ovalbumin showed a significantly abnormal mitochondrial shape and distribution, markedly damaged and widely separated myofibrils with a loss of striations in some of them (Fig. 4h). The examination of the cardiac tissues of the rats in the third group which were sensitized by penicillin G showed a mild damage in myofibrils, a loss of myofibril striations along with abnormal shape and distribution of mitochondria (Fig. 4i).

**Table 1. Comparison between mean  $\pm$  SD of anaphylaxis biomarkers in the different rat groups**

Group Parameter	First M $\pm$ S.D	Second M $\pm$ S.D	Third M $\pm$ S.D	F
Tryptase (ug/l)	2.941 $\pm$ 0.43	7.115 $\pm$ 0.55*	4.995 $\pm$ 0.52**	347.150
IgE (ug/l)	0.3285 $\pm$ 0.02	24.19 $\pm$ 3.22*	11.32 $\pm$ 2.05**	586.269
Histamine (ug/ml)	0.0265 $\pm$ 0.01	0.0895 $\pm$ 0.02*	0.0582 $\pm$ 0.01**	98.029

Number of subjects per group: 20; IgE: Immunoglobulin E; M  $\pm$  S.D: mean  $\pm$  standard deviation; F: The value of the difference between the groups. The first control group received 0.5 ml of distilled water. The second group was sensitized by ovalbumin. The third group was sensitized by penicillin G, \*P < 0.001 (significant difference in comparison to the first group), \*\*P < 0.001 (significant difference in comparison to the second group)

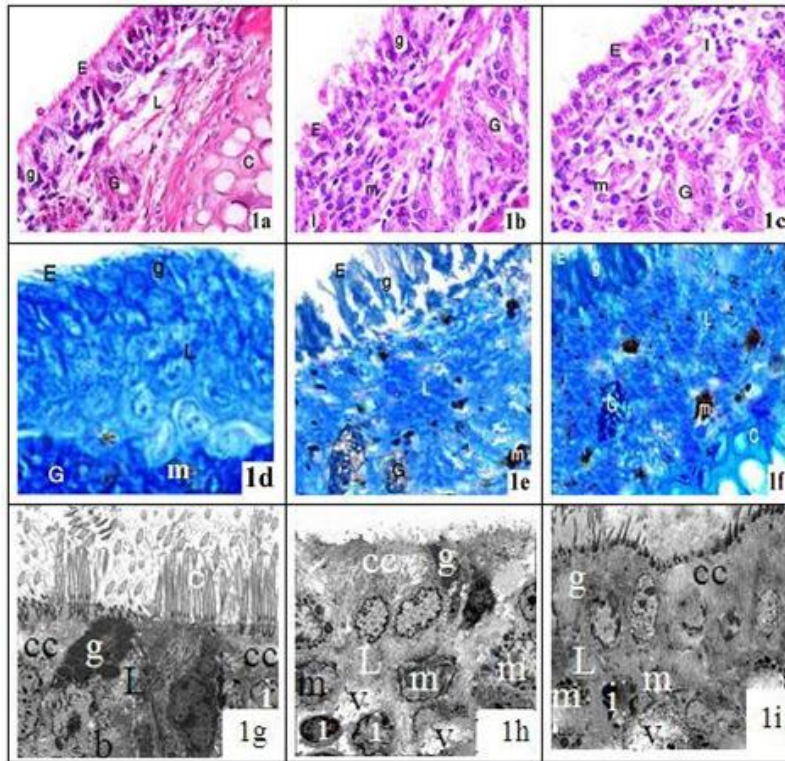


**Fig. 1.** (a) Photomicrograph of a transverse section of a control rat larynx showing a typical pseudostratified ciliated columnar epithelium (E), goblet cells (g) with large masses of the gland (G) and cartilage (C) in the sub- endothelial lamina propria (L). (haematoxylin and eosin (H&E) X200). (b) Photomicrograph of a transverse section of a second group rat larynx showing severe inflammatory cell infiltration (I), epithelial destruction (E), submucosal gland swelling (G), and severe submucosal mast cell infiltration (m). (haematoxylin and eosin (H&E) X200). (c) Photomicrograph of a transverse section in the third group rat larynx showing mild inflammatory cellular infiltration (I), epithelial thickening (E) with submucosal gland swelling (G), and mature mast cells (m). (haematoxylin and eosin (H&E) X200). (d) Photomicrograph of a transverse section of a control rat larynx showing the lining pseudostratified ciliated columnar epithelium (E) and goblet cells (g) with a normal distribution of mast cells (m) around the blood vessels in the subendothelial lamina propria (L). (Toluidine blue X1000). (e) Photomicrograph of a transverse section of a second group rat larynx showing severe epithelial destruction (E), goblet cells destruction (g), submucosal gland swelling (G) in the subendothelial lamina propria (L) with a marked increase in the number of granulated and degranulated mast cells (m). (Toluidine blue X1000). (f) Photomicrograph of a transverse section in the third group larynx showing mild epithelial destruction (E), submucosal gland swelling (G) in the subendothelial lamina propria (L) with a mild increase in the number of granulated and degranulated mast cells (m). (Toluidine blue X1000). (g) Electron microscopic picture of a control rat larynx showing ciliated cells (CC) and cilia (C) with mucus-producing cells (g) and basal cells (b) in the intact epithelial layer along with a few lymphocytes (i) in the connective tissue of the sub-endothelial lamina propria (L). (X10000). (h) Electron microscopic picture of a second group rat larynx showing severe destruction in the epithelium (CC) and the goblet cells (g) with severe cellular infiltration (i) in the sub-endothelial lamina propria (L) and marked increase in the granulated and degranulated mast cells (m). (X10000). (i) Electron microscopic picture of a third group rat larynx showing mild destruction in the epithelium (CC) and the goblet cells (g) with mild cellular infiltration (i) in the sub-endothelial lamina propria (L) and a mild increase in the granulated and degranulated mast cells (m) (X10000)

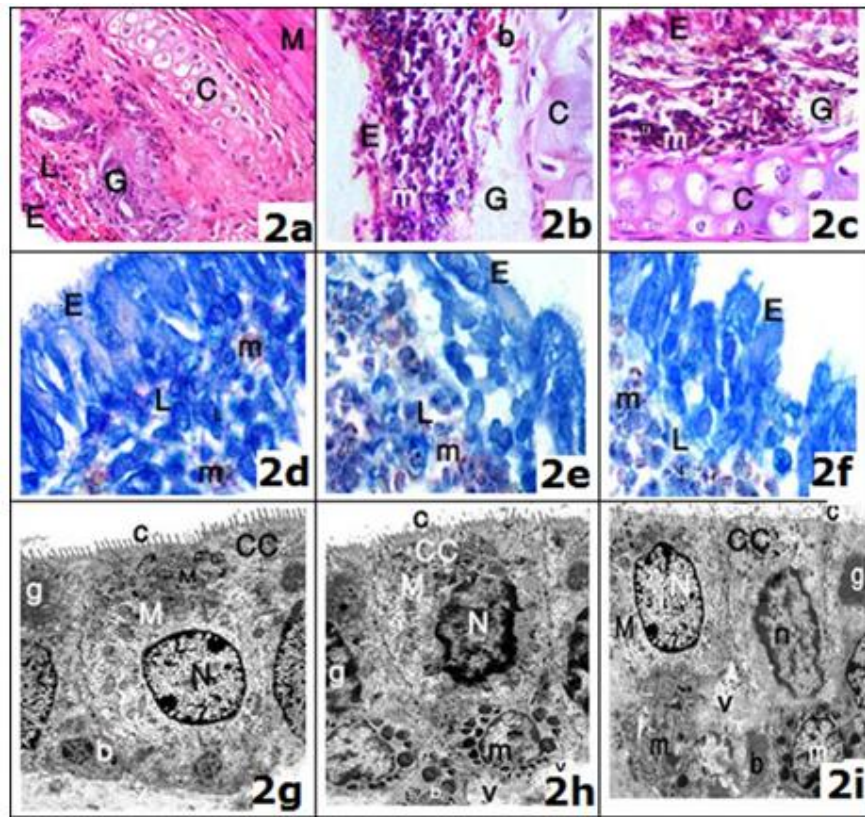


**Fig. 2.** (a) Photomicrograph of a transverse section of a control rat trachea showing normal pseudostratified ciliated columnar epithelium (E), goblet cells (g) with the large masses of the gland (G), cartilage (C) and the muscular trachialis layer (M) in the subendothelial lamina propria (L). (haematoxylin and eosin (H&E) X200). (b) Photomicrograph of a transverse section of a second group rat trachea showing severe epithelial destruction (E), inflammatory cell infiltration (I), submucosal gland swelling (G), and severe mature submucosal granulated and degranulated mast cells (m). (haematoxylin and eosin (H&E) X200). (c) Photomicrograph of a transverse section of a third group rat trachea showing mild epithelial thickening (E) and inflammatory cellular infiltration (I) with submucosal gland swelling (G) and mature submucosal mast cells (m). (haematoxylin and eosin (H&E) X200). (d) Photomicrograph of a transverse section of a control rat trachea showing normal distribution of mast cells (m), classical pseudostratified ciliated columnar epithelium (E) and the subendothelial lamina propria (L). (Toluidine blue X1000). (e) Photomicrograph of a transverse section of a second group rat trachea showing significant increase in the number of the different types of mast cells (m) with a severe epithelial destruction (E). (Toluidine blue X1000). (f) Photomicrograph of a transverse section of a third group trachea showing mild increase in the number of granulated and degranulated mast cells (m) with a mild epithelial destruction (E). (Toluidine blue X1000). (g) Electron microscopic picture of a control rat trachea showing classical appearance of ciliated cells (CC) and cilia (c), normal nucleus (N) and mitochondria (M), mucus-producing cells (g) and basal cells (b). (h) Electron microscopic picture of a second group rat trachea showing severe epithelial destruction (CC), necrotic nuclei (N), destructed mitochondria (M) and basal cells (b), marked increase in the vacuoles (v) and mast cells (m), damaged goblet cells (g) and cilia (c). (X10000). (i) Electron microscopic picture of a third group rat trachea showing mild damage in epithelium (CC), cilia (c), goblet cells (g), basal cells (b), mitochondria (M), and necrotic nuclei (N) along with a low number of vacuoles (v) and mast cells (m) (X10000)

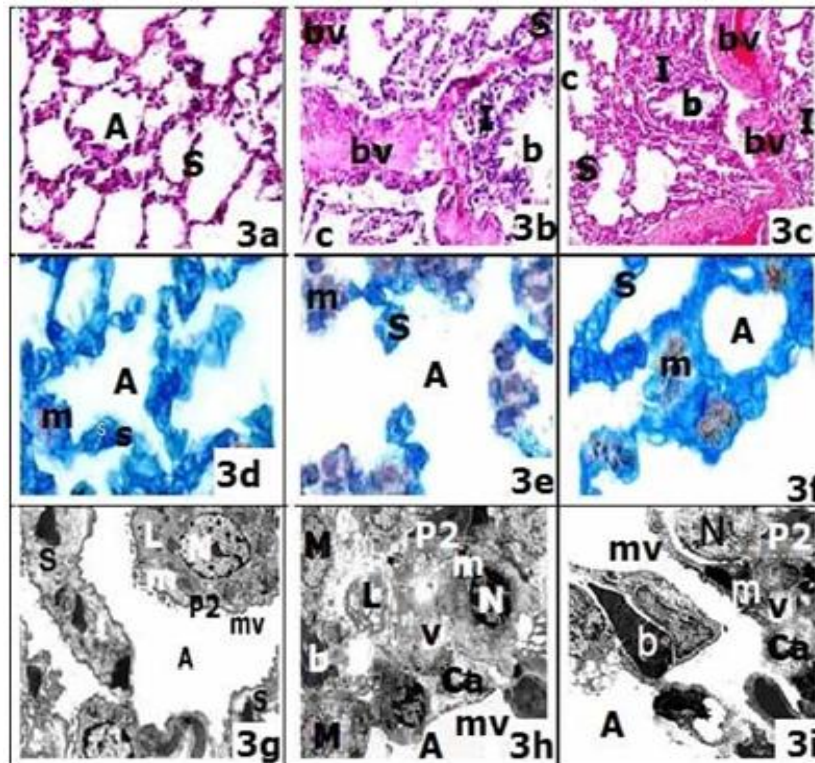


**Fig. 3. (a)** Photomicrograph of a transverse section of a control rat lung showing normal alveoli (A) and thin interalveolar septa (S). (haematoxylin and eosin (H&E) X200). **(b)** Photomicrograph of a transverse section in the second group rat lung showing severe loss of the normal pulmonary architecture, marked collapse of some alveoli (c), marked thickening of interalveolar septum (S), numerous areas of cellular infiltration (I) in the connective tissue surrounding the lung bronchioles (b) with multiple congested blood vessels (bv). (haematoxylin and eosin (H&E) X200). **(c)** Photomicrograph of a transverse section of a third group rat lung showing mild damage of normal architecture, a less number of the collapsed alveoli (c), numerous areas of cellular infiltration (I) surrounding the lung bronchioles (b) and a less number of congested blood vessels (bv). (haematoxylin and eosin (H&E) X200). **(d)** Photomicrograph of a transverse section of a control rat lung showing normal alveoli (A), thin interalveolar septa (S) and a normal distribution of mast cells (m) around the lung blood vessels. (Toluidine blue X1000). **(e)** Photomicrograph of a transverse section of a second group rat lung showing marked increase in the number of mast cells (m) around the lung blood vessels. (Toluidine blue X1000). **(f)** Photomicrograph of a transverse section of a third group lung showing moderate increase in the number of granulated and degranulated mast cells (m) with a less number of the collapsed alveoli (A). (Toluidine blue X1000). **(g)** Electron microscopic picture of a control rat lung showing normal microvilli (mv) on the surface of alveoli (A) with thin interalveolar septa(S), mitochondria (m) in the cytoplasm, rounded nucleus (N) of pneumocyte type II (P2) and the lamellar bodies (L) around the nucleus. **(h)** Electron microscopic picture of a second group rat lung showing collapsed alveoli (Ca) with degenerated microvilli (mv) on the surface of alveoli (A), pyknotic nucleus (N) of pneumocyte type II (P2), degenerated mitochondria (m) and lamellar bodies (L) in cytoplasm, a variable number of vacuoles (v), more congested blood capillaries filled with the blood (b) and a significant increase in total granulated and degranulated mast cells. (X12000). **(i)** Electron microscopic picture of a third group rat lung showing mildly degenerated microvilli (mv) on the surface of alveoli (A), a moderate pyknotic nucleus (N) of pneumocyte type II (P2), mild degenerated mitochondria (m) and lamellar bodies (L), vacuoles (v), less congested blood capillaries filled with the blood (b) and a mild increase in total granulated and degranulated mast cells (X12000)



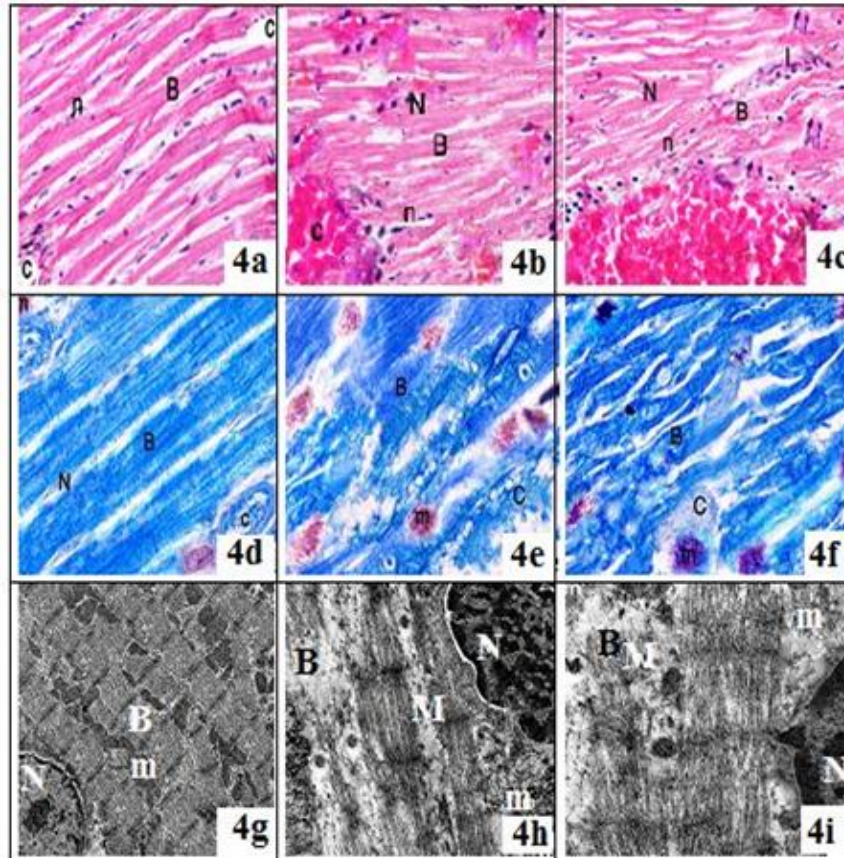


**Fig. 4.** (a) Photomicrograph of a transverse section of a control rat heart showing normal branching and anastomosis cardiac muscle fibers (B), normal central vesicular nuclei (n) and coronary blood vessels (c). (haematoxylin and eosin (H&E) X400). (b) Photomicrograph of a transverse section of a second group rat heart showing the congested and degenerated myocardial fibers (B), a maximum number of necrotic nuclei (N) along with a less number of normal nuclei (n), and the numerous areas of cellular infiltration (I) surrounding the coronary arteries (c). (haematoxylin and eosin (H&E) X400). (c) Photomicrograph of a transverse section of a third group rat heart showing moderate congestion and degeneration in the myocardial fibers (B), normal nuclei (n) along with a less number of necrotic nuclei (N), and the small areas of cellular infiltration (I) surrounding the coronary arteries (c). (haematoxylin and eosin (H&E) X400). (d) Photomicrograph of a transverse section of a control rat heart showing normal cardiac muscle fibers (B), central vesicular nuclei (n) and coronary blood vessels (c) with a normal distribution of mast cells (m) around the blood vessels (Toluidine blue X1000). (e) Photomicrograph of a transverse section of a second group rat heart showing severe increase in the number of mast cells (m) around the congested coronary vessels (c) in the degenerated myocardial fibers (B). (Toluidine blue X1000). (f) Photomicrograph of a transverse section of a third group heart showing mild increase in the number of granulated and degranulated mast cells (m) around the coronary vessels (C) in the degenerated myocardial fibers (B). (Toluidine blue X1000). (g) Electron microscopic picture of a control rat heart showing normal alternating dark and light bands (B) in myofibrils with the rows of mitochondria (M) and nucleus (N) in-between. (X10000). (h) Electron microscopic picture of a second group rat heart showing marked degenerative changes in myocardial fibers (B), significant abnormal mitochondria (M), necrotic nuclei (N) and marked increase in the mast cells (m). (X10000). (i) Electron microscopic picture of a third group rat heart showing mild degenerative changes in myocardial fibers (B) and mitochondria (M), necrotic nuclei (N) and a mild increase in the mast cells (m) (X10000)

### **3.3.5 Spleen**

The examination of the spleens of the control group rats showed a classic appearance of the nucleus and organelles (Fig. 5g). The examination of the spleens of the second group rats which were sensitized by ovalbumin showed a severe blood sinusoidal stasis in the red pulp, macrophage, lymphocyte, and mast cell infiltration with cytoplasmic vacuoles in some erythrocytes (Fig. 5h). The examination of the spleens of the third group rats which were sensitized by penicillin G showed mild mitochondrial swelling, dilated rough endoplasmic reticulum, erythrocytes and eosinophils in the venous sinusoids with vacuoles in the cytoplasm of some cells (Fig. 5i).

## **4. DISCUSSION**

Postmortem diagnosis of fatal anaphylaxis is considered a complicated issue for forensic experts because of the various causes of anaphylaxis and its effect on a large number of body systems. Hence, this study has tried to diagnose induced fatal anaphylaxis in rats postmortem, depending on specific and comprehensive criteria including biochemical, immunological and histological findings instead of focusing on the exclusion of the other causes of sudden death.

This study showed that there is a statistically significant increase in the total serum levels of tryptase and immunoglobulin E (IgE), and the blood histamine level in the second group that was sensitized by ovalbumin in comparison to the control group and the third group that were sensitized by penicillin G. According to George and Caughey [19], serum mast cell tryptase and IgE are considered the biomarkers of mast cell activation in the different organs of anaphylaxis cases which is consistent with [20] that showed that the release of sensitive and specific markers such as tryptase from the mast cells stimulated by allergens, along with an increase in specific IgE levels proved antemortem sensitization. In addition to this, Salkie and his colleagues [21] clarified that the levels of immunoglobulin E (IgE) and tryptase are stable in the postmortem serum for several weeks; thus according to [22], anaphylaxis may be diagnosed as a cause of sudden death, based on the levels of immunoglobulin E (IgE) and tryptase that rise in parallel with increasing postmortem interval. Similarly, Simons [23] showed that specific IgE can be identified based on the most common

causes of fatal anaphylaxis such as food or penicillin that is considered one of the iatrogenic agents. In our study, the biomarker values are significantly different between the second and third group, which is in agreement with [24] that showed that this difference is related to the cause and severity of anaphylaxis.

Edston and Van Hage-Hamsten [25] indicated that the increase in postmortem total tryptase level often correlates with an increase in the histamine level which is another indicator of mast cell degranulation. According to Lieberman and Li [26,27], histamine is considered one of the major mediators of anaphylaxis despite its short half-life wherein it declines to the baseline within one hour because of its rapid metabolism. Thus, the high histamine level may support the diagnosis of anaphylaxis, which is consistent with our results. However, Edston and Van Hage-Hamsten [28] demonstrated that the postmortem serum tryptase level or histamine level may rise in cases where sudden death is attributed to other causes such as trauma; thus according to [29,30], the postmortem serum tryptase level and histamine level are considered nonspecific markers for anaphylaxis diagnosis without other supporting findings.

Our results showed a significant increase in the number of granulated and degranulated mast cells of the different organs of the rats in the second group that were sensitized by ovalbumin in comparison to those of the control group and the third group that was sensitized by penicillin G, which is in agreement with Fineschi et al. [31] who confirmed that there is an increase in the number of mast cells in fatal anaphylactic shock and the increase varies depending on the cause of anaphylaxis. Similarly, Lieberman et al. [32] clarified that the high levels of tryptase may be correlated with an increase in the number of mast cells, especially the degranulated type supporting the anaphylaxis diagnosis. Edston et al. [33] indicated that there is no correlation between the high level of tryptase and the increase in the number of mast cells; however, in agreement with [34], anaphylaxis may be associated with granulated or degranulated mast cells according to whether the cause of anaphylaxis is allergic or non-allergic.

The current study noted severe histopathological and ultrastructural changes in the upper and lower airways of the larynx, trachea and lungs of the rats in the second group that were sensitized by ovalbumin. But, these changes were lesser in severity in the third group that was sensitized by

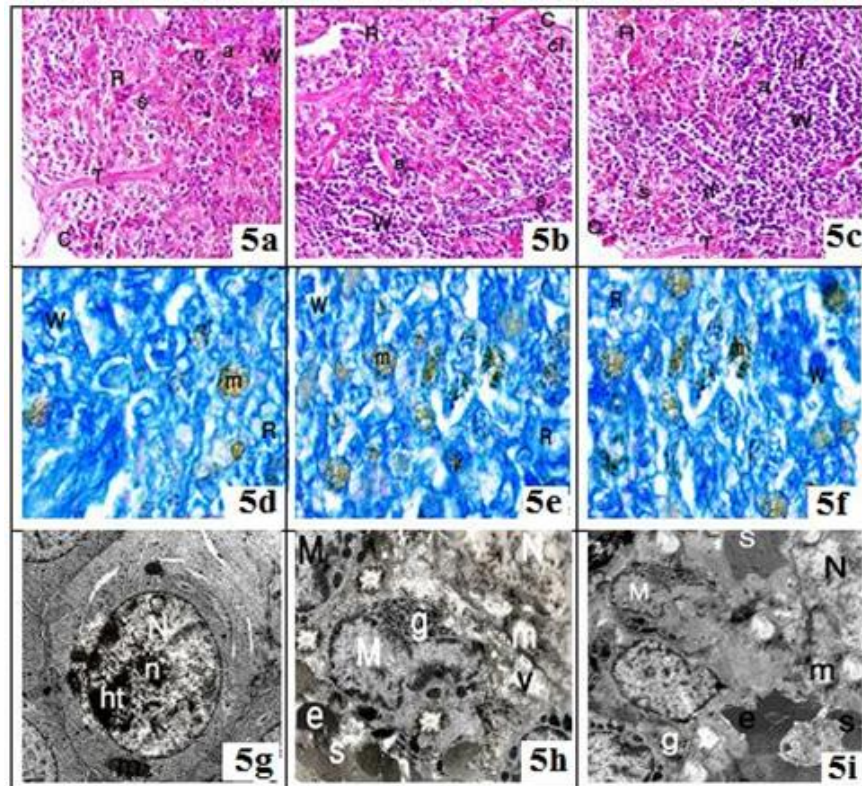


**Fig. 5.** (a) Photomicrograph of a transverse section of a control rat spleen showing normal capsule (C), trabeculae (T), white pulp (W) and red pulp (R), central artery (a) in the white pulp, lymphoid nodule (n) and the marginal zone (m), and the splenic blood sinuses (s). (haematoxylin and eosin (H&E) X200). (b) Photomicrograph of a transverse section of a second group rat spleen showing the hyalinized capsule (c) and trabeculae (T), lymphocytic infiltration (if) with subcapsular cloudy swelling (cl), marked congestion and dilatation of the splenic blood sinuses (s) in the red pulp (R), hyalinosis in the wall of central arterioles (a) and white pulp destruction (W). (haematoxylin and eosin (H&E) X200). (c) Photomicrograph of a transverse section of a third group rat spleen showing capsule (c), trabeculae (T), mild lymphocytic infiltration (if), hemorrhage, mild congestion and dilatation of splenic blood sinuses (s) in the red pulp (R) with vacuolated cytoplasm in the white (W) and red (R) pulp, and hyalinosis in the wall of central arterioles (a). (haematoxylin and eosin (H&E) X200). (d) Photomicrograph of a transverse section of a control rat spleen showing normal mast cells distribution (m) around the blood vessels. (Toluidine blue X1000). (e) Photomicrograph of a transverse section of a second group rat spleen showing a severe increase in the mast cells (m) around the blood vessels with the vacuolated cytoplasm in the white pulp (W) and dilatation in the splenic blood sinuses of the red pulp (R). (Toluidine blue X1000). (f) Photomicrograph of a transverse section of a third group spleen showing mild increase in the granulated and degranulated mast cells (m) with a mild vacuolated cytoplasm in the white pulp (W), and the splenic blood sinuses dilatation in the red pulp (R). (Toluidine blue X1000). (g) Electron microscopic picture of a control rat spleen showing normal nucleolus (n), nucleus (N), heterochromatin (ht), and mitochondria (m). (X8000). (h) Electron microscopic picture of a second group rat spleen showing severe vacuolation in the nucleus (N), mitochondria (m) and cytoplasm (v) of lymphocyte with an increase in the number of erythrocytes (e) and the granulated and degranulated (g) mast cells (M) around the sinusoidal area (s). (X12000). (i) Electron microscopic picture of a third group rat spleen showing a mild vacuolation in the nucleus (N), mitochondria (m) and cytoplasm (v) of lymphocyte with a mild increase in the number of erythrocytes (e) and the granulated and degranulated (g) mast cells (M) around the sinusoidal area (s) (X12000)

penicillin G in comparison to the second group. These histopathological changes are consistent with the results of [35] which indicated that there is increased upper and lower airway resistance during anaphylactic shock due to obstructions via edema, congestion, and mucous plugging that lead to breathing difficulty resulting in asphyxia and respiratory arrest, which is in agreement with the opinions of [36,37]. According to Pumphrey and Roberts [38], the severity of upper and lower respiratory histopathological changes depends on multiple factors such as the allergen type, the route of administration and the time passed between exposure and death. This explains our results that show a difference in the severity degree of histological changes between the second and the third group which used two different allergen types. However, Horn [8] and others showed that there are no specific airways histological changes in fatal anaphylactic shock and then postmortem diagnosis must be integrated with other findings.

Regarding the heart, many histopathological and ultrastructural changes were observed in the second group which was sensitized by ovalbumin, such as severe damage in cardiac architecture, degeneration of myocardial fibers along with significantly abnormal mitochondria and marked cellular infiltration. These cardiac changes were lesser in severity in the third group that was sensitized by penicillin G in comparison to the second group. Our results are in agreement with [39] which found that cardiac arrest may occur as the direct effect of anaphylaxis mediators on the heart, leading to histological changes based on the time between exposure and death or may immediately follow the respiratory arrest while Lu et al. [40] showed that the mode of death may be different for each cause of anaphylaxis. Our results are also consistent with Kounis et al. [41] who confirmed that anaphylaxis leads to myocardial damage along with the inflammatory process causing cardiac histopathological changes.

The present study observed serious histopathological and ultrastructural changes in the spleen of the second group that was sensitized by ovalbumin, such as capsule and central arterioles hyalinization, severe lymphocytic and macrophage infiltration, mitochondrial swelling with cytoplasmic vacuolization in erythrocytes, dilation of the blood sinuses and rough endoplasmic reticulum, hemorrhage and congestion in the red pulp, and white pulp atrophy. These changes were of

moderate severity in the third group that was sensitized by penicillin G in comparison to the second group. The studies in [42,43] suggested that non-specific postmortem findings in systemic anaphylaxis are usually due to generalized mast cell degranulation which is attributed to an immunological reaction leading to the release of mediators from the mast cells causing vasodilatation along with an increase in vascular permeability, and then a generalized congestion and edema in the different body organs such as the spleen which is in agreement with [44,45,46] that showed that the mast cell quantification in splenic red pulp and serum tryptase assessment may help diagnose fatal anaphylactic shock with a high degree of sureness.

## 5. CONCLUSION

Postmortem diagnosis of fatal anaphylaxis depends on a multi-factorial criteria which includes biochemical, immunological, and histological findings such as increases in the levels of total tryptase, histamine and immunoglobulin E (IgE) along with non-specific histopathological changes in larynx, trachea, lung, heart, and spleen that vary in its severity depending on the cause of anaphylaxis. Further research in humans is recommended to verify our results.

## COMPETING INTERESTS

Authors have declared that no competing interests exist.

## REFERENCES

1. Simons FE. Anaphylaxis. *J Allergy Clin Immunol.* 2010;125(2):161-81.
2. Edston E, Van Hage-Hamsten M. Diagnosis of anaphylaxis in: *Forensic pathology reviews*, Humana Press Inc, Totowa, New Jersey. 2005;3(6):267-281.
3. Klotz JH, Klotz SA, Pinnas JL. Animal Bites And Stings With Anaphylactic Potential. *J Emerg Med.* 2009;36(2):148-56.
4. Greenberger PA, Rotskoff BD, Lifschultz B. Fatal anaphylaxis: Postmortem findings and associated comorbid diseases. *Annals of Allergy, Asthma & Immunology.* 2007; 98(3):252-257.
5. Johann-Liang R, Josephs S, Dreskin SC. Analysis of anaphylaxis cases after vaccination: 10-year review from the

- national vaccine injury compensation. *Annals of Allergy, Asthma, and Immunology*. 2011;106(5):440-443.
6. Richard SHP, Ian SDR. Postmortem findings after fatal anaphylactic reactions. *J Clin Pathol*. 2000;53(4):273-276.
  7. Benede S, Blazquez AB, Chiang D, Tordesillas L and Berin MC. The rise of food allergy: Environmental factors and emerging treatments. *EBiomed*. 2016; 7(1):27-34.
  8. Horn KD, Halsey JF, Zumwalt RE. Utilization of serum tryptase and immunoglobulin E assay in the postmortem diagnosis of anaphylaxis. *The American Journal of Forensic Medicine and Pathology*. 2004;25(1):37-43.
  9. Byard RW. Anaphylaxis at autopsy, Editorial. *Forensic Sci Med Pathol*. Epub. Aug 29, 2016;(1-3).  
DOI: 10.1007/s12024-016-9799-4
  10. Shibamoto T, Cui S, Ruan Z, Liu W, Takano H, Kurata Y. Hepatic venoconstriction is involved in anaphylactic hypotension in rats. *Am J Physiol Heart Circ Physiol*. 2005;289(1):1436-1441.
  11. Dhar HL, Kulkarnid N. Cross reactivity of cephalosporins with penicillin. *Indian J Physiol. Phannacol*. 1994;38(4):303-305.
  12. Schwartz LB, Bradford TR, Rouse C. Development of a new, more sensitive immunoassay for human tryptase: Use in systemic anaphylaxis. *J Clin Immunol*. 1994;14(3):190-204.
  13. Schwartz LB. Diagnostic value of tryptase in anaphylaxis and mastocytosis. *Immunol Allergy Clin North Am*. 2006;26(1):451-463.
  14. McBride P, Bradley D, Kaliner M. Evaluation of a radioimmunoassay for histamine measurement in biologic fluids. *J Allergy and Clinical Immunology*. 1988; 82(4):638-646.
  15. Chi DS, Fitzgerald SM, Krishnaswamy G. Mast cell histamine and cytokine assays. *Methods Mol Biol*. 2006;315(1):203-15.
  16. Wang J, Godbold JH, Sampson HA. Correlation of serum allergy (IgE) tests performed by different assay systems. *J Allergy Clin Immunol*. 2008;121(5):1219-1224.
  17. Bancroft JD, Gamble M. *Theory and Practice Histological Techniques*, 5th ed., Churchill Livingstone. New York, Edinburgh and London. 2002;126 and 173-175.
  18. Graham L, Orenstein JM. Processing tissue and cells for transmission electron microscopy in diagnostic pathology and research. *Nat Protoc*. 2007;2(10):2439-50.
  19. George H, Caughey MD. Tryptase genetics and anaphylaxis. *J Allergy Clin. Immunol*. 2006;117(6):1411-1414.
  20. Herbst J, Heath K, Heddle R, Gilbert JD, Byard RW. Multiple bee stings, peritumoral mast cell degranulation and anaphylaxis - is there a relationship? *J Forensic Leg Med*. 2013;20(1):591-4.
  21. Salkie ML, Mitchell I, Revers CW, Karkhanis A, Butt J, Tough S, Green FH. Postmortem serum levels of tryptase and total and specific IgE in fatal asthma. *Allergy Asthma Proc*. 1998;19(3):131-3.
  22. Byard RW. *Sudden death in the young*. 3rd ed., Cambridge, UK: Cambridge University Press. 2010;649-655.
  23. Simons FE. Anaphylaxis pathogenesis and treatment. *Allergy*. 2011;66(95):31-34.
  24. Brown SGA, Stone SF. Laboratory diagnosis of acute anaphylaxis. *Clin. Exp. Allergy*. 2011;41(1):1660-1662.
  25. Edston E, Van Hage-Hamsten M. â-Tryptase measurements post-mortem in anaphylactic deaths and controls. *Forensic Sci. Int*. 1998;93(1):135-42.
  26. Lieberman PL. Anaphylaxis; in Adkinson NF Jr., Bochner BS, Busse WW, Holgate ST, Lemanske RF Jr., Simons FER (eds): *Middleton's Allergy: Principles and Practice*, ed 7. St. Louis, Mosby. 2009; 1027-1049.
  27. Li Z, Gao Y, Wang H, Liu Z. A rat model of Shuang Huang Lian injection-induced anaphylaxis. *Asian Pac J Allergy Immunol*. 2010;28(2):185-191.
  28. Edston E, Van Hage-Hamsten M. Mast cell tryptase and hemolysis after trauma. *Forensic Sci Int*. 2003;131(1):8-13.
  29. Sala-Cunill A, Cardona V, Labrador-Horrillo M, Luengo O, Estes O, Garriga T, Vicario M, Guilarte M. Usefulness and Limitations of Sequential Serum Tryptase for the Diagnosis of Anaphylaxis in 102 Patients. *Int Arch Allergy Immunol*. 2013; 160(2):192-199.
  30. Belsey SL, Flanagan RJ. Postmortem biochemistry: Current applications. *J Forensic Leg Med*. 2016;41(1):49-57.
  31. Fineschi V, Cecchi R, Centini F, Paglicci Reattelli L, Turillazzi E. Immunohistochemical quantification of pulmonary mast cells and post-mortem blood dosages of tryptase and eosinophil

- cationic protein in 48 heroin-related deaths. *Forensic Sci Int.* 2001;120(3):189-194.
32. Lieberman P, Nicklas RA, Oppenheimer J, Kemp SF, Lang DM, et al. The diagnosis and management of anaphylaxis practice parameter: Update. *The Journal of Allergy and Clinical Immunology.* 2010; 126 (3):477-480.
  33. Edston E, Eriksson O, Van Hage M. Mast cell tryptase in postmortem serum reference values and confounders, *International Journal of Legal Medicine.* 2007;121(4):275- 280.
  34. Munoz-Cano R, Picado C, Valero A and Bartra J. Mechanisms of anaphylaxis beyond IgE. *J Invest. Aller. Clin. Immunol.* 2016;26(2):73-82.
  35. Da Broi U, Moreschi C. Post-mortem diagnosis of anaphylaxis: A difficult task in forensic medicine. *Forensic Science International.* 2011;204(1-3):1-5.
  36. Riches KJ, Byard RW. The detection of fatal anaphylaxis at autopsy - an overview. *Scand J Forensic Sci.* 2004;10(1):61-3.
  37. Brown SGA, Stone SF, Fatovich DM, Burrows SA, Holdgate A, Celenza A, et al. Anaphylaxis: Clinical patterns, mediator release, and severity. *J Allergy Clin. Immunol.* 2013;132(5):1141-1149.
  38. Pumphrey RSH, Roberts ISD. Postmortem findings after fatal anaphylactic reactions. *J Clin. Pathol.* 2000;53(4):273-276.
  39. Low I, Stables S. Anaphylactic deaths in Auckland, New Zealand: a review of coronial autopsies from 1985 to 2005. *Pathology.* 2006;38(4):328-332.
  40. Lu P, Bao CS, Wang LX. Analysis on 27 autopsy cases died of anaphylactic shock induced by mainline. *Fa Yi Xue Za Zhi.* 2006;22(4):305-306.
  41. Kounis NG, Kounis GN, Soufras GD, Lianas D, Patsouras N. Postmortem diagnosis of drug- induced anaphylactic death: Kounis syndrome and hypersensitivity myocarditis are the likely culprit in death of severe anaphylactic reactions. *J Forensic Leg Med.* 2016; 40(1):40-1.
  42. Shepherd GM. Hypersensitivity reactions to drugs: evaluation and management. *Mt. Sinai J Med.* 2003;70(2):113-25.
  43. Osawa M, Satoh F, Horiuchi H, Tian W, Kugota N, Hasegawa I. Postmortem diagnosis of fatal anaphylaxis during intravenous administration of therapeutic and diagnostic agents: Evaluation of clinical laboratory parameters and immunohistochemistry in three cases. *Legal Medicine.* 2008;10(3):143-147.
  44. Radheshi E, Bonetti LR, Confortini A, Silingardi E, Palmiere C. Postmortem diagnosis of anaphylaxis in presence of decompositional changes. *Journal of Forensic and Legal Medicine.* 2016;38(1): 97-100.
  45. Reggiani BL, Maccio L, Trani N, Radheshi E, Palmiere C. Splenic hypereosinophilia in anaphylaxis-related death: different assessments depending on different types of allergens? *Int J Leg Med.* 2015; 129(1):97-103.
  46. Palmiere C, Comment L, Vilarino R, Mangin P, Reggiani Bonetti L. Measurement of  $\beta$ -tryptase in postmortem serum in cardiac deaths. *J Forensic Leg Med.* 2014;23(1):12-18.

© 2018 Elshama et al.; This is an Open Access article distributed under the terms of the Creative Commons Attribution License (<http://creativecommons.org/licenses/by/4.0>), which permits unrestricted use, distribution, and reproduction in any medium, provided the original work is properly cited.

*Peer-review history:*

*The peer review history for this paper can be accessed here:*  
<http://www.sciencedomain.org/review-history/23020>